

## Highly Luminescent Poly(Methyl Methacrylate)-Incorporated Europium Complex Supported by a Carbazole-Based Fluorinated $\beta$ -Diketonate Ligand and a 4,5-Bis(diphenylphosphino)-9,9-dimethylxanthene Oxide Co-Ligand

D. B. Ambili Raj,<sup>†</sup> Biju Francis,<sup>†</sup> M. L. P. Reddy,<sup>\*,†</sup> Rachel R. Butorac,<sup>‡</sup> Vincent M. Lynch,<sup>‡</sup> and Alan H. Cowley<sup>‡</sup>

<sup>†</sup>Chemical Sciences and Technology Division, National Institute for Interdisciplinary Science & Technology (NIIST), CSIR, Thiruvananthapuram-695 019, India, and <sup>‡</sup>Department of Chemistry and Biochemistry, The University of Texas at Austin, 1 University Station A5300, Austin, Texas 78712

Received July 30, 2010

A novel efficient antenna complex of  $\text{Eu}^{3+}$  [ $\text{Eu}(\text{CPFHP})_3(\text{DDXPO})$ ] supported by a highly fluorinated carbazole-substituted  $\beta$ -diketonate ligand, namely, 1-(9H-carbazol-2-yl)-4,4,5,5,5-pentafluoro-3-hydroxypent-2-en-1-one (CPFHP) and the 4,5-bis(diphenylphosphino)-9,9-dimethylxanthene oxide (DDXPO) ancillary ligand, has been synthesized, structurally characterized, and its photoluminescent behavior examined. The single-crystal X-ray diffraction analysis of  $\text{Eu}(\text{CPFHP})_3(\text{DDXPO})$  revealed that this complex is mononuclear, and that the central  $\text{Eu}^{3+}$  ion is surrounded by eight oxygen atoms, six of which are provided by the three bidentate  $\beta$ -diketonate ligands. The remaining two oxygen atoms are furnished by the chelating phosphine oxide ligand. The coordination polyhedron is best described as that of a distorted square antiprism. The photophysical properties of  $\text{Eu}(\text{CPFHP})_3(\text{DDXPO})$  benefit from adequate protection of the metal by the ligands with respect to non-radiative deactivation as well as an efficient ligand-to-metal energy transfer process which exceeds 66% in chloroform solution with a quantum yield of 47%. As an integral part of this work, the synthesis, characterization, and luminescent properties of poly(methyl methacrylate) (PMMA) polymer films doped with  $\text{Eu}(\text{CPFHP})_3(\text{DDXPO})$  are also reported. The luminescent efficiencies of the doped films (photoluminescence quantum yields 79–84%) are dramatically enhanced in comparison with that of the precursor complex. The new luminescent PMMA-doped  $\text{Eu}(\text{CPFHP})_3(\text{DDXPO})$  complex therefore shows considerable promise for polymer light-emitting diode and active polymer optical fiber applications.

### Introduction

The unique photoluminescent properties of europium complexes render them appropriate for a host of applications, such as display devices, solid state lighting (including OLEDs), and sensors.<sup>1–3</sup> The shielding of the f orbitals by the  $5s^2$  and  $5p^6$  closed shells results in narrow line-like emissions of optically pure colors with long radiative lifetimes. However, the f-f transitions that result in light emission from the lanthanides are both spin- and parity-forbidden which, in turn, mandates the use of antenna molecules for indirect excitation of the metal center. This indirect excitation, also known as the

antenna effect, takes advantage of the coordinated ligands in the sense that energy transfer from the ligand-centered excited states to the metal center results in lanthanide ion luminescence.<sup>4</sup> In 1942, Weissman observed that the use of organic ligands in europium complexes increased the luminescence intensity from the lanthanide ion when such complexes were irradiated with ultraviolet (UV) light.<sup>5</sup> The  $\beta$ -diketone ligand class is emerging as one of the important “antennas” in terms of high harvest emissions because of the effectiveness of the energy transfer from this ligand type to the  $\text{Ln}^{3+}$  cation.<sup>6</sup>

It is well documented that the replacement of the C–H bonds of a  $\beta$ -diketone ligand with lower-energy C–F oscillators is capable of lowering the vibrational energy of the ligand.<sup>7</sup> In turn, this decreases the energy loss because of ligand vibration and therefore enhances the emission intensity

\*To whom correspondence should be addressed. E-mail: mlpreddy55@gmail.com.

(1) (a) Kido, J.; Okamoto, Y. *Chem. Rev.* **2002**, *102*, 2357–2368. (b) de Bettencourt-Dias, A. *Dalton Trans.* **2007**, 22, 2229–2241. (c) Bünzli, J.-C. G.; Piguet, C. *Chem. Soc. Rev.* **2005**, *34*, 1048–1077.

(2) (a) Kuriki, K.; Koike, Y.; Okamoto, Y. *Chem. Rev.* **2002**, *102*, 2347–2356. (b) Polman, A.; van Veggel, F. C. G. M. *J. Opt. Soc. Am. B* **2004**, *21*, 871–892.

(3) (a) Fernandez-Moreira, V.; Song, B.; Sivagnanam, V.; Chauvin, A.-S.; Vandevyver, C. D. B.; Gijss, M.; Hemmila, I.; Lehr, H.-A.; Bünzli, J.-C. G. *Analyst* **2010**, *135*, 42–52. (b) Eliseeva, S. V.; Bünzli, J.-C. G. *Chem. Soc. Rev.* **2010**, *39*, 189–227. (c) Bünzli, J.-C. G. *Chem. Rev.* **2010**, *110*, 2729–2755.

(4) (a) Lehn, J. M. *Angew. Chem., Int. Ed.* **1990**, *29*, 1304–1319. (b) Sabbatini, N.; Guardiglia, M.; Lehn, J. M. *Coord. Chem. Rev.* **1993**, *123*, 201–228. (c) Piguet, C.; Bünzli, J.-C. G. *Chem. Soc. Rev.* **1999**, *28*, 347–358. (d) Petoud, S.; Cohen, S. M.; Bünzli, J.-C. G.; Raymond, K. N. *J. Am. Chem. Soc.* **2003**, *125*, 13324–13325.

(5) Weissman, S. I. *J. Chem. Phys.* **1942**, *10*, 214.

of the lanthanide ion.<sup>8</sup> Furthermore, because of the heavy-atom effect, which facilitates intersystem crossing, the lanthanide-centered luminescent properties are also improved.<sup>1c,9</sup> In recent years, the carbazole functional group has been incorporated into  $\beta$ -diketonate ligands to improve the hole transport mobility of lanthanide complexes.<sup>10</sup> Carbazoles possess a number of other desirable properties which include good chemical and environmental stability, modest cost, and the ability to tune the optical and electrical properties by substitution with a wide variety of functional groups.<sup>11</sup> It was consideration of these factors that prompted us to design and synthesize the new  $\beta$ -diketonate ligand, 1-(9*H*-carbazol-2-yl)-4,4,5,5,5-pentafluoro-3-hydroxypent-2-en-1-one, which features both a polyfluorinated alkyl group and a carbazole unit.

Chelated lanthanide  $\beta$ -diketonate complexes typically are isolated with two water molecules incorporated in the first coordination sphere of the central metal ion. Unfortunately, the presence of such water molecules quenches the lanthanide emission by activation of non-radiative decay pathways.<sup>12</sup> One way to circumvent this problem is to replace the water molecules with ancillary ligands bearing chromophores that are capable of playing the antenna role. An additional requirement in this regard is that the antenna ligand should bind sufficiently strongly to the lanthanide center that the coordination of water molecules is precluded. In selecting the ancillary ligand, attention needs to be paid to enhancing the volatility and thermal stability as well as to the film forming properties and the carrier transport behavior. Given the

foregoing considerations, a significant number of lanthanide tris( $\beta$ -diketonates) have been prepared that also feature coordinated bidentate nitrogen<sup>13</sup> and phosphine oxide<sup>14</sup> ligands. Such complexes have been reported to serve as efficient light conversion molecular devices. Consideration of the foregoing results motivated us to design the new europium antenna complex, Eu(CPFHP)<sub>3</sub>(DDXPO), which contains a highly fluorinated carbazole-substituted  $\beta$ -diketonate, namely, 1-(9*H*-carbazol-2-yl)-4,4,5,5,5-pentafluoro-3-hydroxypent-2-en-1-one (CPFHP). The coordination sphere also contains 4,5-bis-(diphenylphosphino)-9,9-dimethylxanthene oxide (DDXPO) as an ancillary ligand. The newly synthesized Eu<sup>3+</sup> complex was characterized on the basis of elemental analysis, <sup>1</sup>H and <sup>13</sup>C NMR, and mass spectroscopy.

Recent years have witnessed a growing interest in lanthanide-polymer complexes because of the combination of the good luminescent properties of lanthanide complexes and the excellent mechanical processing properties of polymers.<sup>15</sup> Typical applications for such polymer films are as organic light emitting diodes<sup>16</sup> (OLEDs) or as active optical polymer fibers for data transmission.<sup>17</sup> A popular polymer matrix for use as a host for luminescent lanthanide complexes is poly(methyl methacrylate) (PMMA) which is a low-cost, simply prepared polymer of excellent optical quality. This material is transparent at wavelengths longer than 250 nm.<sup>18</sup> In the present work, we report the synthesis and photophysical properties of the new Eu<sup>3+</sup> complex, [Eu(CPFHP)<sub>3</sub>(DDXPO)] which exhibits excellent quantum yield values (79–84%) in PMMA. The overall aim of this work was to develop a simple and feasible method for the production of a luminescent material with the objective of obtaining information about the photoluminescence (PL) behavior of the optical material incorporated into the polymer film. The sensitization effect of the polymer matrixes on the Eu<sup>3+</sup> luminescent center is discussed in detail based on excitation and emission spectra, luminescence decay curves, experimental intensity parameters, and quantum yields.

(6) (a) Binnemans, K. *Chem. Rev.* **2009**, *109*, 4283–4374. (b) Ambili Raj, D. B.; Biju, S.; Reddy, M. L. P. *Inorg. Chem.* **2008**, *47*, 8091–8100. (c) Remya, P. N.; Biju, S.; Reddy, M. L. P.; Cowley, A. H.; Findlater, M. *Inorg. Chem.* **2008**, *47*, 7396–7404. (d) Biju, S.; Reddy, M. L. P.; Cowley, A. H.; Vasudevan, K. V. *Cryst. Growth Des.* **2009**, *9*, 3562–3569. (e) Biju, S.; Ambili Raj, D. B.; Reddy, M. L. P.; Jayasankar, C. K.; Cowley, A. H.; Findlater, M. *J. Mater. Chem.* **2009**, *19*, 1425–1432. (f) Ambili Raj, D. B.; Biju, S.; Reddy, M. L. P. *Dalton Trans.* **2009**, *36*, 7519–7528. (g) Ambili Raj, D. B.; Biju, S.; Reddy, M. L. P. *J. Mater. Chem.* **2009**, *19*, 7976–7983. (h) Divya, V.; Biju, S.; Luxmi Varma, R.; Reddy, M. L. P. *J. Mater. Chem.* **2010**, *20*, 5220–5227. (i) Biju, S.; Reddy, M. L. P.; Cowley, A. H.; Vasudevan, K. V. *J. Mater. Chem.* **2009**, *19*, 5179–5187.

(7) (a) Hasegawa, Y.; Ohkubo, T.; Sogabe, K.; Kawamura, Y.; Wada, Y.; Nakashima, N.; Yanagida, S. *Angew. Chem., Int. Ed.* **2000**, *39*, 357–360. (b) Glover, P. B.; Bassett, A. P.; Nockemann, P.; Kariuki, B. M.; Deun, R. V.; Pikramenou, Z. *Chem.—Eur. J.* **2007**, *13*, 6308–6320.

(8) (a) Batista, H. J.; de Andrade, A. V. M.; Longo, R. L.; Simas, A. M.; de Sá, G. F.; Nao, K. I.; Thompson, L. C.; Chauvin, A.-S.; Gummy, F.; Matsubayashi, I.; Yuko Hasegawa, Y.; Bünzli, J.-C. G. *Eur. J. Inorg. Chem.* **2006**, 473–480. (b) Sun, L.-N.; Yu, J.-B.; Zheng, G.-L.; Zhang, H.-J.; Meng, Q.-G.; Peng, C.-Y.; Fu, L.-S.; Liu, F.-Y.; Yu, Y.-N. *Eur. J. Inorg. Chem.* **2006**, 3962–3973.

(9) Hasegawa, Y.; Wada, Y.; Yanagida, S. *J. Photochem. Photobiol., C* **2004**, *5*, 183–202.

(10) (a) Baek, N. S.; Kim, Y. H.; Eom, Y. K.; Oh, J. H.; Kim, H. K.; Aebischer, A.; Gummy, F.; Chauvin, A.-S.; Bünzli, J.-C. G. *Dalton Trans.* **2010**, *39*, 1532–1538. (b) Zheng, Y.; Cardinali, F.; Armaroli, N.; Accorsi, G. *Eur. J. Inorg. Chem.* **2008**, 2075–2080. (c) Nie, D.; Chen, Z.; Bian, Z.; Zhou, J.; Liu, Z.; Chen, F.; Zhao, Y.; Huang, C. *New J. Chem.* **2007**, *31*, 1639–1646. (d) He, P.; Wang, H. H.; Liu, S. G.; Shi, J. X.; Wang, G.; Gong, M. L. *Inorg. Chem.* **2009**, *48*, 11382–11387.

(11) (a) Grazulevicius, J. V.; Strohriegel, P.; Pielichowski, J.; Pielichowski, K. *Prog. Polym. Sci.* **2003**, *28*, 1297–1353. (b) Morin, J. F.; Leclerc, M.; Ades, D.; Siove, A. *Macromol. Rapid Commun.* **2005**, *26*, 761–778.

(12) de Sa, G. F.; Malta, O. L.; de Mello Donega, C.; Simas, A. M.; Longo, R. L.; Santa-Cruz, P. A.; da Silva, E. F., Jr. *Coord. Chem. Rev.* **2000**, *196*, 165–195.

(13) (a) Biju, S.; Ambili Raj, D. B.; Reddy, M. L. P.; Kariuki, B. M. *Inorg. Chem.* **2006**, *45*, 10651–10660. (b) Bellusci, A.; Barberio, G.; Crispini, A.; Ghedini, M.; La Deda, M.; Pucci, D. *Inorg. Chem.* **2005**, *44*, 1818–1825. (c) Law, G.-L.; Wong, K.-L.; Tam, H.-L.; Cheah, K.-W.; Wong, W.-T. *Inorg. Chem.* **2009**, *48*, 10492–10494. (d) Chen, X. Y.; Bretonniere, Y.; Pecaut, J.; Imbert, D.; Bunzli, J.-C. G.; Mazzanti, M. *Inorg. Chem.* **2007**, *46*, 625–637.

(14) (a) Xu, H.; Wang, L.-H.; Zhu, X.-H.; Yin, K.; Zhong, G.-Y.; Hou, X.-Y.; Huang, W. *J. Phys. Chem. B* **2006**, *110*, 3023–3029. (b) Xu, H.; Yin, K.; Huang, W. *ChemPhysChem* **2008**, *9*, 1752–1760. (c) Xu, H.; Yin, K.; Huang, W. *Chem.—Eur. J.* **2007**, *13*, 10281–10293. (d) Xu, H.; Yin, K.; Huang, W. *J. Phys. Chem. C* **2010**, *114*, 1674–1683.

(15) (a) McGehee, M. D.; Bergstedt, T.; Zhang, C.; Saab, A. P.; O'Regan, M. B.; Bazan, G. C.; Srdanov, V. I.; Heeger, A. J. *Adv. Mater.* **1999**, *11*, 1349–1354. (b) Balamurugan, A.; Reddy, M. L. P.; Jayakannan, M. *J. Phys. Chem. B* **2009**, *113*, 14128–14138. (c) Boyer, J. C.; Johnson, N. J. J.; van Veggel, F. C. J. M. *Chem. Mater.* **2009**, *21*, 2010–2012. (d) Kai, J.; Parrab, D. F.; Brito, H. F. J. *Mater. Chem.* **2008**, *18*, 4549–4554. (e) Zhang, H.; Song, H.; Dong, B.; Han, L.; Pan, G.; Bai, X.; Fan, L.; Lu, S.; Zhao, H.; Wang, F. *J. Phys. Chem. C* **2008**, *112*, 9155–9162.

(16) (a) Yu, J.; Zhou, L.; Zhang, H.; Zheng, Y.; Li, H.; Deng, R.; Peng, Z.; Li, Z. *Inorg. Chem.* **2005**, *44*, 1611–1618. (b) Liang, F.; Zhou, Q.; Cheng, Y.; Wang, L.; Ma, D.; Jing, X.; Wang, F. *Chem. Mater.* **2003**, *15*, 1935–1937. (c) Shunmugam, R.; Tew, G. N. *J. Am. Chem. Soc.* **2005**, *127*, 13567–13572. (d) Chen, X.-Y.; Yang, X.; Holliday, B. J. *J. Am. Chem. Soc.* **2008**, *130*, 1546–1547.

(17) (a) Klink, S. I.; Grave, L.; Reinhoudt, D. N.; van Veggel, F. C. J. M.; Werts, M. H. V.; Geurts, F. A. J.; Hofstraat, J. W. *J. Phys. Chem. A* **2000**, *104*, 5457–5468. (b) McGehee, M. D.; Bergstedt, T.; Zhang, C.; Saab, A. P.; O'Regan, M. B.; Bazan, G. C.; Srdanov, V. I.; Heeger, A. J. *Adv. Mater.* **1999**, *11*, 1349–1354.

(18) (a) Hasegawa, Y.; Yamamuro, M.; Wada, Y.; Kanehisa, N.; Kai, Y.; Yanagida, S. *J. Phys. Chem. A* **2003**, *107*, 1697–1702. (b) Lunstrook, K.; Driesen, K.; Nockemann, P.; Viau, L.; Mutin, P. H.; Vioux, A.; Binnemans, K. *Phys. Chem. Chem. Phys.* **2010**, *12*, 1879–1885. (c) Fan, W.-Q.; Feng, J.; Song, S.-Y.; Lei, Y.-Q.; Zheng, G.-L.; Zhang, H.-J. *Chem.—Eur. J.* **2010**, *16*, 1903–1910.

## Experimental Section

**Materials and Instrumentation.** Europium(III) nitrate hexahydrate of 99.9% purity and 4,5-bis(diphenylphosphino)-9,9-dimethylxanthene of 97% purity were purchased from Treibacher and Alfa-Aesar, respectively. Gadolinium(III) nitrate hexahydrate, 2-acetylcarbazole (98% purity), methyl pentafluoropropionate (99% purity), and sodium hydride (60% dispersion in mineral oil) were procured from Sigma-Aldrich. All the other chemicals used were of analytical reagent grade. The bidentate phosphine oxide, 4,5-bis(diphenylphosphino)-9,9-dimethylxanthene oxide (DDXPO), was synthesized according to the method described in an earlier publication.<sup>6f</sup>

The C, H, and N elemental analyses were performed on a Perkin-Elmer Series 2 Elemental Analyzer 2400. The IR spectra were recorded as KBr pellets on a Perkin-Elmer Spectrum One FT-IR spectrometer operating between 450 and 400 cm<sup>-1</sup>. A Bruker 500 MHz NMR spectrometer was used to record the <sup>1</sup>H NMR (300 MHz), <sup>13</sup>C NMR (125.7 MHz), and <sup>31</sup>P NMR (202.4 MHz) spectra of the new compounds in chloroform-d or acetone-d<sub>6</sub> solution. The chemical shifts are reported in parts per million relative to tetramethylsilane, SiMe<sub>4</sub> for <sup>1</sup>H NMR and <sup>13</sup>C NMR spectra and with respect to 85% phosphoric acid for <sup>31</sup>P NMR spectra. The mass spectra were recorded on a JEOL JSM 600 fast atom bombardment (FAB) high resolution mass spectrometer (FAB-MS), and the thermogravimetric analyses were performed on a TG/DTA-6200 instrument (SII Nano Technology Inc., Japan). UV-absorption spectra were recorded with a Shimadzu, UV-2450 UV-vis spectrophotometer. All spectra were corrected for the background spectrum of the solvent. The absorbances of the ligands and complexes were measured in CHCl<sub>3</sub> solution. The PL spectra were recorded on a Spex-Fluorolog FL22 spectrofluorimeter equipped with a double grating 0.22 m Spex 1680 monochromator and a 450W Xe lamp as the excitation source operating in the front face mode. The lifetime measurements were carried out at room temperature using a Spex 1040 D phosphorimeter.

The overall quantum yields of the sensitized Eu<sup>3+</sup> emissions of the complexes were measured in CHCl<sub>3</sub> solution at room temperature and are cited relative to a reference solution of quinine sulfate in 1 N H<sub>2</sub>SO<sub>4</sub> ( $\phi = 54.6\%$ ). Corrections were made for the refractive index of the solvent. All solvents were of spectroscopic grade. The overall luminescent quantum yields of the complexes were calculated according to the well-known equation,<sup>19</sup>

$$\phi_{\text{overall}} = \frac{n^2 A_{\text{ref}} I}{n_{\text{ref}}^2 A I_{\text{ref}}} \phi_{\text{ref}} \quad (1)$$

where  $n$ ,  $A$ , and  $I$  denote the refractive index of solvent, the area of the emission spectrum, and the absorbance at the excitation wavelength, respectively, and  $\phi_{\text{ref}}$  represents the quantum yield of the standard quinine sulfate solution. The subscript *ref* denotes the reference, and the absence of a subscript implies an unknown sample. The refractive index is assumed to be equivalent to that of the pure solvent: 1.45 for chloroform and 1.33 for water at room temperature.

The overall quantum yields for the Eu<sup>3+</sup> doped films were determined under ligand excitation (330–420 nm) and are based on the absolute method using a calibrated integrating sphere in a

**Table 1.** Crystallographic and Refinement Data for Complex 2

parameters	2
formula	C <sub>96</sub> H <sub>75</sub> EuF <sub>15</sub> N <sub>3</sub> O <sub>13</sub> P <sub>2</sub>
fw	1977.49
cryst syst	monoclinic
space group	<i>P21/n</i>
cryst size, mm <sup>3</sup>	0.1 × 0.1 × 0.09
temp/K	100(2)
<i>a</i> (Å)	11.4888(11)
<i>b</i> (Å)	33.356(3)
<i>c</i> (Å)	22.684(2)
$\alpha$ (deg)	90
$\beta$ (deg)	96.751(3)
$\gamma$ (deg)	90
<i>V</i> (Å <sup>3</sup> )	8632.6(14)
<i>Z</i>	4
<i>D</i> <sub>calcd</sub> , Mg/m <sup>3</sup>	1.522
$\mu$ (Mo, K $\alpha$ ), mm <sup>-1</sup>	0.863
F(000)	4016.0
R1 [ <i>I</i> > 2 $\sigma$ ( <i>I</i> )]	0.0823
wR2 [ <i>I</i> > 2 $\sigma$ ( <i>I</i> )]	0.1580
R1 (all data)	0.1609
wR2 (all data)	0.1810
GOF	1.054

SPEX Fluorolog spectrofluorimeter. A Xe-arc lamp was used to excite the thin-film samples placed in the sphere. The quantum yield was determined by comparing the spectral intensities of the lamp and the sample emission as reported in the literature.<sup>20</sup> Using this experimental setup and the integrating sphere system, the solid-state fluorescence quantum yield of a thin film of the standard green OLED material tris-8-hydroxyquinolinolato aluminum (Alq<sub>3</sub>) was determined to be 0.19, which is consistent with previously reported values.<sup>21</sup> Each sample was measured several times under slightly different experimental conditions. The estimated error for the quantum yields is ( $\pm 10\%$ ).<sup>22</sup>

The X-ray diffraction data were collected on a Rigaku AFC-12 Saturn 724+ CCD diffractometer equipped with a graphite-monochromated Mo K $\alpha$  radiation source ( $\lambda = 0.71073$  Å) and a Rigaku XStream low temperature device cooled to 100 K. Corrections were applied for Lorentz and polarization effects. The structure was solved by direct methods and refined by full-matrix least-squares cycles on *F*<sup>2</sup> using the Siemens SHELXTL PLUS 5.0 (PC) software package<sup>23a</sup> and PLATON.<sup>23b</sup> All non-hydrogen atoms were refined anisotropically, and the hydrogen atoms were placed in fixed, calculated positions using a riding model. Selected crystal data and data collection and refinement parameters are listed in Table 1. Two of the C<sub>2</sub>F<sub>5</sub> groups in complex 2 display a typical disorder, which has been modeled and refined successfully. X-ray crystallographic information files can be obtained free of charge via [www.ccdc.cam.ac.uk/const/retrieving.html](http://www.ccdc.cam.ac.uk/const/retrieving.html) (or from CCDC, 12 Union Road, Cambridge CB2 1EZ, U.K.; fax, +44 1223 336033; e-mail, [deposit@ccdc.cam.ac.uk](mailto:deposit@ccdc.cam.ac.uk)). The CCDC number for the Eu(CPFHP)<sub>3</sub>(DDXPO) complex is CCDC 771380.

**Synthesis of 1-(9H-Carbazol-2-yl)-4,4,5,5,5-pentafluoro-3-hydroxy-pent-2-en-1-one (CPFHP).** A modification of the typical Claisen condensation procedure was used for the synthesis of CPFHP as shown in Scheme 1. 2-Acetylcarbazole (0.002 mmol) and methyl pentafluoropropionate (0.002 mmol) were dissolved in 20 mL of anhydrous tetrahydrofuran (THF) under a N<sub>2</sub>

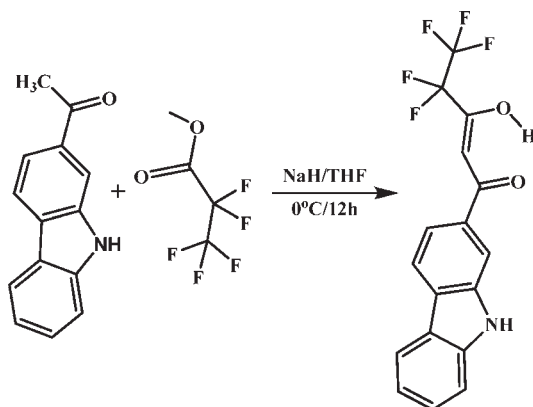
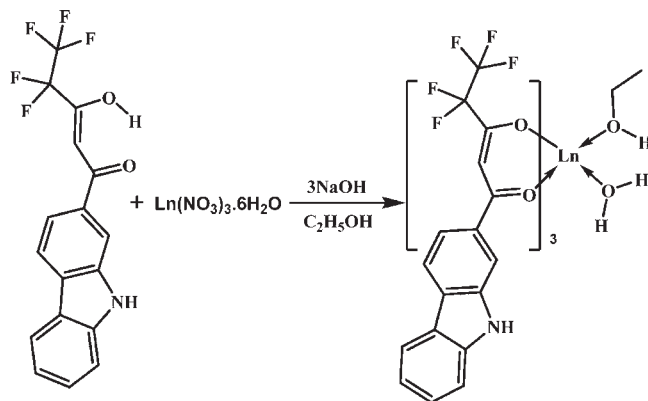
(19) (a) Eaton, D. F. *Pure Appl. Chem.* **1988**, *60*, 1107–1114. (b) Demasa, J. N.; Crosby, G. A. *J. Phys. Chem.* **1971**, *76*, 991–1024. (c) Meech, S. R.; Phillips, D. J. *Photochem.* **1983**, *23*, 193–217. (d) Werts, M. H. V.; Jukes, R. T. F.; Verhoeven, J. W. *Phys. Chem. Chem. Phys.* **2002**, *4*, 1542–1548.

(20) (a) Wrighton, M. S.; Ginley, D. S.; Morse, D. L. *J. Phys. Chem.* **1974**, *78*, 2229. (b) Palsson, L.-O.; Monkman, A. P. *Adv. Mater.* **2002**, *14*, 757–758. (c) Shah, B. K.; Neckers, D. C.; Shi, J.; Forsythe, E. W.; Morton, D. *Chem. Mater.* **2006**, *18*, 603–608. (d) De Mello, C.; Wittmann, H. F.; Friend, R. H. *Adv. Mater.* **1997**, *9*, 230–232.

(21) (a) Colle, M.; Gmeiner, J.; Milius, W.; Hillebrecht, H.; Brütting, W. *Adv. Funct. Mater.* **2003**, *13*, 108–112. (b) Saleesh Kumar, N. S.; Varghese, S.; Rath, N. P.; Das, S. J. *Phys. Chem. C* **2008**, *112*, 8429–8437.

(22) Eliseeva, S. V.; Kotova, O. V.; Gumy, F.; Semenov, S. N.; Kessler, V. G.; Lepnev, L. S.; Bünzli, J.-C. G.; Kuzmina, N. P. *J. Phys. Chem. A* **2008**, *112*, 3614–3626.

(23) (a) Sheldrick, G. M. *SHELXTL-PC*, Version 5.03; Siemens Analytical X-ray Instruments, Inc.: Madison, WI, 1994. (b) Spek, A. L. *Acta Crystallogr., Sect. A* **1990**, *C34*, 46.

**Scheme 1.** Synthesis of the CPFHP Ligand**Scheme 2.** Synthesis of Ln(CPFHP)<sub>3</sub>(H<sub>2</sub>O)(C<sub>2</sub>H<sub>5</sub>OH) [Ln = Eu<sup>3+</sup> (1) or Gd<sup>3+</sup> (3)]

atmosphere, and the temperature was maintained at 0 °C. Sodium hydride was added, and the reaction mixture was stirred for 12 h, following which it was quenched with water. Hydrochloric acid (2.0 M) was then added, and the resulting mixture was extracted with CH<sub>2</sub>Cl<sub>2</sub> and dried over anhydrous Na<sub>2</sub>SO<sub>4</sub>. The residue was purified by column chromatography (chloroform/hexane = 1:4) to give the final product as a yellowish solid (yield 65%). Elemental analysis (%): Calcd for C<sub>17</sub>H<sub>10</sub>F<sub>5</sub>NO<sub>2</sub> (355.26): C, 57.47; H, 2.84; N, 3.94. Found: C, 57.73; H, 3.17; N, 3.98. <sup>1</sup>H NMR (500 MHz, chloroform-d): δ (ppm) 15.57 (broad, enol -OH), 8.36 (s, 1H), 8.17–8.13 (m, 3H), 7.83–7.81 (dd, 1H, *J* = 1.5 Hz, *J* = 1.5 Hz), 7.55–7.50 (m, 2H), 7.32–7.29 (m, 1H), 6.77 (s, 1H). <sup>13</sup>C NMR (125 MHz, acetone-d<sub>6</sub>): δ (ppm) 186.72, 178.06–177.64, 142.95–142.81, 140.51–140.37, 140.09, 130.12, 129.22–128.71, 122.96, 122.92, 122.31–121.97, 121.57–121.23, 120.62–120.15, 119.49–119.29, 118.15, 112.42–112.09, 109.01, 94.62. FT-IR (KBr) ν<sub>max</sub>: 3346, 2923, 2853, 1630, 1580, 1203, 1173, 1118, 1018, 804 cm<sup>-1</sup>. *m/z* = 356.76 (M+H)<sup>+</sup>.

**Synthesis of Ln(CPFHP)<sub>3</sub>(C<sub>2</sub>H<sub>5</sub>OH)(H<sub>2</sub>O) [Ln = Eu<sup>3+</sup> (1), Gd<sup>3+</sup> (3)].** A mixture of the β-diketonate ligand CPFHP (0.6 mmol) and NaOH (0.6 mmol) in an acetone-ethanol solvent mixture was stirred for 10 min at room temperature, following which a saturated ethanolic solution of Ln(NO<sub>3</sub>)<sub>3</sub>·6H<sub>2</sub>O (0.2 mmol) was added dropwise, and the reaction mixture was stirred subsequently for 10 h. Water was then added, and the precipitate that had formed was filtered off, washed with water, dried and purified by recrystallization from an acetone-water mixture (Scheme 2). Elemental analysis (%): Calcd for C<sub>53</sub>H<sub>35</sub>F<sub>15</sub>O<sub>8</sub>-N<sub>3</sub>Eu (1) (1278.81): C, 49.78; H, 2.76; N, 3.29. Found: C, 49.97; H, 2.54; N, 3.07. FT-IR (KBr) ν<sub>max</sub>: 3418, 2924, 1603, 1529, 1469, 1327, 1259, 1166, 1013, 750 cm<sup>-1</sup>. *m/z* = 1233.65 (M<sup>+</sup> - C<sub>2</sub>H<sub>5</sub>OH) + H. Elemental analysis (%): C<sub>53</sub>H<sub>35</sub>F<sub>15</sub>O<sub>8</sub>N<sub>3</sub>Gd (3) (1284.76): C, 49.78; H, 2.76; N, 3.29. Found: C, 50.02; H,

2.61; N, 3.17. FT-IR (KBr) ν<sub>max</sub>: 3423, 2925, 1602, 1528, 1464, 1328, 1277, 1197, 1015, 798 cm<sup>-1</sup>. *m/z* = 1222.89 (M<sup>+</sup> - H<sub>2</sub>O, C<sub>2</sub>H<sub>5</sub>OH) + H.

**Synthesis of Eu(CPFHP)<sub>3</sub>(DDXPO) (2).** Complex 2 was prepared by stirring equimolar quantities of Eu(CPFHP)<sub>3</sub>(H<sub>2</sub>O)(C<sub>2</sub>H<sub>5</sub>OH) and the phosphine oxide DDXPO in CHCl<sub>3</sub> solution for 24 h at room temperature (Scheme 3). The product was isolated by solvent evaporation and purified by recrystallization from a chloroform-hexane mixture. Crystals of complex 2 suitable for single-crystal X-ray diffraction study were obtained upon storage of a saturated solution of the complex in a CHCl<sub>3</sub>/2-methoxy-ethanol solvent mixture. Elemental analysis (%): Calcd for C<sub>90</sub>H<sub>59</sub>EuF<sub>15</sub>N<sub>3</sub>O<sub>9</sub>P<sub>2</sub> (1825.35): C, 59.22; H, 3.26; N, 2.30. Found: C, 59.47; H, 3.24; N, 2.38. FT-IR (KBr) λ<sub>max</sub>: 2924, 1611, 1520, 1404, 1212, 1195, 1173, 1146, 1125, 1070, 1007, 748, 689, 539 cm<sup>-1</sup>; *m/z* = 1470.21 [Eu(CPFHP)<sub>2</sub>(DDXPO) + H].

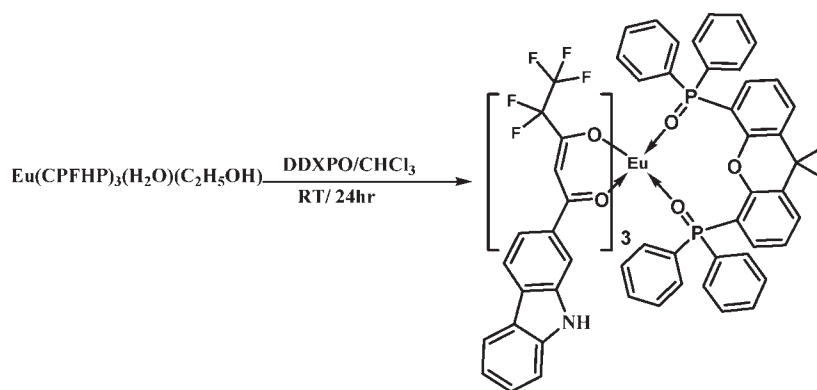
**Synthesis of Eu<sup>3+</sup> Complex-Doped PMMA Polymer Films.** The PMMA polymer was doped with the Eu<sup>3+</sup> complex 2 in the proportions 2.5 (4), 7.5 (5), 10 (6), and 15% (7) (w/w). The PMMA powder was dissolved in chloroform, followed by addition of the required amount of complex 2 in chloroform solution, and the resulting mixture was heated at 40 °C for 30 min. The polymer film was obtained after evaporation of excess solvent at 60 °C.<sup>24</sup>

## Results and Discussion

**Synthesis and Characterization of the CPFHP Ligand and Ln<sup>3+</sup> Complexes 1–3.** The ligand 1-(9H-carbazol-2-yl)-4,4,5,5,5-pentafluoro-3-hydroxypent-2-en-1-one (CPFHP) was synthesized in 65% yield from the corresponding ketone and ester by a modified Claisen condensation reaction. The overall procedure is summarized in Scheme 1. The ligand was characterized by <sup>1</sup>H NMR (Supporting Information, Figure S1), <sup>13</sup>C NMR (Supporting Information, Figure S2), FT-IR, and mass spectroscopic (FAB-MS) methods, as well as by elemental analysis. The lanthanide complexes were prepared as shown in Schemes 2 and 3. The complexes were characterized by FT-IR, mass spectroscopy (FAB-MS), and elemental analyses. The elemental analyses and FAB-MS studies revealed that the central Ln<sup>3+</sup> ion is coordinated to three β-diketonate ligands. In the case of complex 2, one molecule of the bidentate phosphine oxide, DDXPO, is also present in the coordination sphere. The FT-IR spectra of complexes 1 and 3 exhibit a broad absorption in the 3000–3500 cm<sup>-1</sup> region, thereby indicating the presence of solvent molecules in the coordination sphere of the Ln<sup>3+</sup> ion. On the other hand, the absence of this broad band in the 3000–3500 cm<sup>-1</sup> region in the case of complex 2 implied that the solvent molecules had been replaced successfully by the bidentate phosphine oxide ligand. The carbonyl stretching frequency for the CPFHP ligand (1630 cm<sup>-1</sup>) shifted to lower wave numbers in compounds 1–3 (1603 cm<sup>-1</sup> for 1; 1611 cm<sup>-1</sup> for 2; 1602 cm<sup>-1</sup> for 3), thus confirming coordination of the carbonyl oxygen to the Ln<sup>3+</sup> cation in each case. The fact that the P=O stretching frequency of DDXPO at 1180 cm<sup>-1</sup> shifted to 1173 cm<sup>-1</sup> in complex 2 confirms the involvement of the P=O bond of DDXPO in complex formation.

The thermal behavior of the Eu<sup>3+</sup> complexes under a nitrogen atmosphere were examined by means of thermogravimetric analysis (TGA). The general profiles of the

(24) Moudam, O.; Rowan, B. C.; Alamiry, M.; Richardson, P.; Richards, B. S.; Jones, A. C.; Robertson, N. *Chem. Commun.* **2009**, 6649–6651.

Scheme 3. Synthesis of  $\text{Eu}(\text{CPFHP})_3(\text{DDXPO})$ 

weight losses for complexes **1** and **2** are displayed in Supporting Information, Figure S3. It is clear from the TGA data that complex **1** undergoes a mass loss of approximately 5% (Calcd: 5.01%) in the first step (120 to 180 °C), which corresponds to the elimination of the coordinated water and solvent molecules. On the other hand, complex **2** is stable up to 180 °C, above which it decomposes. The final residue for complex **1** is approximately 20% of the initial mass while that for complex **2** is approximately 15%. These residual masses correspond to formation of the non-volatile europium(III) oxyfluoride.

The PMMA polymer was doped with  $\text{Eu}(\text{CPFHP})_3(\text{DDXPO})$  (**2**) in the proportions of 2.5, 7.5, 10, and 15% (w/w) and characterized by FT-IR spectroscopy. The band at  $1726\text{ cm}^{-1}$  for PMMA corresponds to the C=O vibration,<sup>25</sup> whereas for the Eu/PMMA films, this vibration shifts to  $1731\text{ cm}^{-1}$ . In turn, this implies that the  $\text{Eu}^{3+}$  complex is stabilized by means of interactions with the oxygen atoms of the carbonyl group of PMMA. Such interactions might stem from the donation of a pair of electrons from the carbonyl oxygen to the lanthanide ions. The broad absorption band assigned to the  $\text{H}_2\text{O}$  vibrational modes in the FT-IR spectrum of  $\text{Eu}^{3+}$  complex **1**, which appears in the  $3000\text{--}3500\text{ cm}^{-1}$  region, is absent in the doped PMMA polymer films thereby confirming that the polymer films are anhydrous. Such a conclusion is in good agreement with the TG analyses of the doped polymer film, for which no mass loss was observed in the temperature region  $50\text{--}200\text{ }^\circ\text{C}$  (Supporting Information, Figure S4). Both the doped and the undoped films decompose at approximately  $150\text{ }^\circ\text{C}$ .

**X-ray Crystal Structure of  $[\text{Eu}(\text{CPFHP})_3(\text{DDXPO})]$  **2**.** Single crystals of complex **2** suitable for X-ray analysis were grown from a  $\text{CHCl}_3/2$ -methoxy ethanol solution. The crystal structure of **2** was determined by single-crystal X-ray diffraction, and the asymmetric unit is depicted in Figure 1. The crystal data and data collection parameters are presented in Table 1, and selected bond distances and bond angles are summarized in Table 2. The single crystal X-ray analysis reveals that the complex **2** crystallizes in the monoclinic space group  $P21/n$ . The absence of a center of symmetry in **2** results in an increase in the

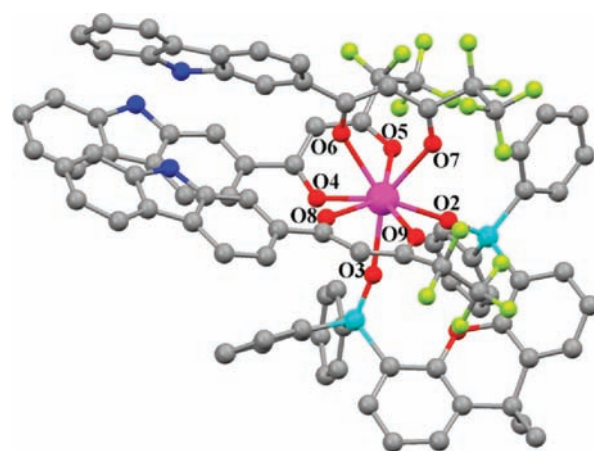


**Figure 1.** Asymmetric unit of complex **2** displayed as a ball and stick model at 25% probability level. All hydrogen atoms have been omitted for clarity.

**Table 2.** Selected Bond Lengths (Å) and Angles (deg) for Complex **2**

Eu (1)–O(2)	2.300(9)
Eu (1)–O(3)	2.372(10)
Eu (1)–O(4)	2.345(7)
Eu (1)–O(5)	2.414(7)
Eu (1)–O(6)	2.400(9)
Eu (1)–O(7)	2.411(10)
Eu (1)–O(8)	2.399(11)
Eu (1)–O(9)	2.358(12)
O(2)–Eu (1)–O(3)	73.0(3)
O(4)–Eu (1)–O(5)	70.75(19)
O(6)–Eu (1)–O(7)	69.6(3)
O(8)–Eu (1)–O(9)	69.9(4)

number of electronic transitions of the 4f orbitals because of the odd parity.<sup>26</sup> An Oak Ridge thermal ellipsoid plot (ORTEP) view of **2** reveals an eight-coordinate  $\text{Eu}^{3+}$  cation environment comprising one chelated phosphine oxide (DDXPO) and three bidentate fluorinated  $\beta$ -diketonate ligands. The coordination polyhedron can best be described as that of a distorted square antiprism. The central  $\text{Eu}^{3+}$  ion is surrounded by bulky carbazole-substituted fluorinated  $\beta$ -diketonates and bidentate chelating phosphine oxide ligands. This encapsulated structure therefore meets the structural requirements for an efficient lanthanide luminescent material since the  $\text{Eu}^{3+}$  ion is protected from vibrational coupling thereby increasing the light absorption cross-section by the so-called “antenna

(25) Liu, H.-G.; Lee, Y.-I.; Qin, W.-P.; Jang, K.; Kim, S.; Feng, X.-S. *J. Appl. Polym. Sci.* **2004**, *92*, 3524–3530.

(26) Hasegawa, Y.; Yamamuro, M.; Wada, Y.; Kanehisa, N.; Kai, Y.; Yanagida, S. *J. Phys. Chem. A* **2003**, *107*, 1697–1702.

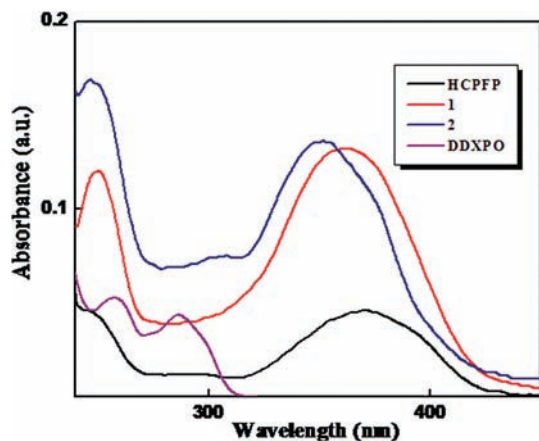


**Figure 2.** UV-vis absorption spectra of the ligands CPFHP and DDXPO and complexes **1** and **2** in  $\text{CHCl}_3$  solution ( $c = 2 \times 10^{-6} \text{ mol dm}^{-3}$ ).

effect". It is interesting to note that the bridging oxygen atom that connects the two triphenylphosphine oxide units of the chelated phosphine oxide is not coordinated to the central  $\text{Eu}^{3+}$  ion. The two  $\text{Eu}-\text{O}$  bonds of the chelated phosphine oxide ligand (2.30 Å and 2.37 Å) are shorter than the six  $\text{Eu}-\text{O}$  bonds of the fluorinated  $\beta$ -diketonate ligands (2.34 Å–2.41 Å). A similar trend is evident in the single-crystal X-ray data for the complex  $\text{Eu}^{3+}$ -hexafluoroacetylacetonato-1,1'-biphenyl-2,2'-diylbis(diphenylphosphine oxide) [ $\text{Eu}-\text{O}$  bond distances 2.32–2.33 Å in BIPHEPO and 2.40–2.44 Å in the  $\beta$ -diketonate].<sup>27</sup> Thus the chelating phosphine oxide DDXPO coordinates more strongly to the  $\text{Eu}^{3+}$  ion than the  $\beta$ -diketonate ligands. Furthermore, in the case of DDXPO, the two diphenylphosphine oxide units are linked by a xanthene moiety that increases the extent of conjugation in the chelating ligand. In turn, this serves to improve the carrier injection and transport properties of **2**. Moreover, the introduction of a more conjugated DDXPO ligand renders the complex more rigid, which in turn reduces the structural relaxation in the excited state.<sup>6f,28</sup>

**Electronic States of the Ligands.** The UV-visible absorption spectra of the free ligands (CPFHP and DDXPO) and their corresponding  $\text{Eu}^{3+}$  complexes (**1** and **2**) in  $\text{CHCl}_3$  solution ( $c = 2 \times 10^{-6} \text{ mol dm}^{-3}$ ) are displayed in Figure 2. The trends in the absorption spectra of these complexes are identical to the ones observed for the free ligands, indicating that the singlet excited states of the ligands are not significantly affected by the complexation to the  $\text{Eu}^{3+}$  ion. However, a small blue shift that is attributable to the perturbation induced by metal coordination. The ligand CPFHP displays a composite broad band in the UV corresponding to a singlet–singlet  $\pi-\pi^*$  enolic transition assigned to the  $\beta$ -diketonate moiety,<sup>6</sup> with a lowest energy maximum at 315–440 nm ( $\lambda_{\text{max}} = 370 \text{ nm}$ ) and a molar absorption coefficient of  $2.3 \times 10^4 \text{ L M}^{-1} \text{ cm}^{-1}$ . The higher energy absorption bands detected in the range 240–270 nm are attributable to the  $\pi-\pi^*$  transi-

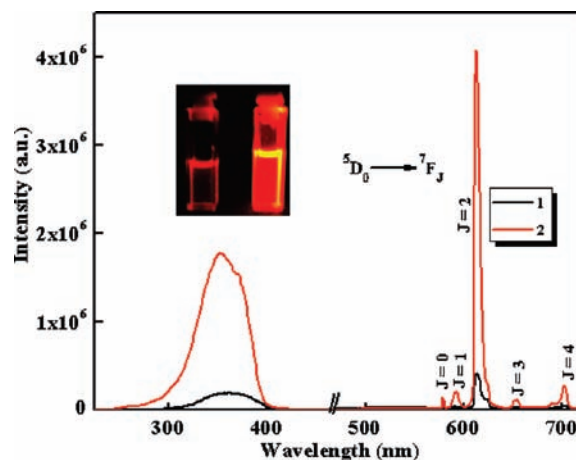


**Figure 3.** Room temperature (303 K) excitation and emission spectra of complexes **1** and **2** in  $\text{CHCl}_3$  solution ( $c = 1.5 \times 10^{-6} \text{ mol dm}^{-3}$ ).

tion of the locally excited state of the carbazole moiety of the  $\beta$ -diketonate ligand.<sup>10c</sup> The electronic transitions of the  $\beta$ -diketonate (peak at ca. 240–270 nm) and the chelated phosphine oxide (peak at ca. 248–270 nm) units are overlapped by the carbazole features.<sup>10b</sup> The presence of the ancillary ligand DDXPO not only enhances the absorption intensity but also satisfies the high coordination number of the central  $\text{Eu}^{3+}$  ion and thus improves the coordination and thermal stabilities of complex **2**. The molar absorption coefficient values for **1** and **2** were calculated at the respective  $\lambda_{\text{max}}$  value and were found to be  $6.68 \times 10^4$  and  $6.75 \times 10^4 \text{ L mol}^{-1} \text{ cm}^{-1}$ , respectively. The magnitudes of these values are approximately three times higher than that of the  $\beta$ -diketonate ligand, and this trend is consistent with the presence of three  $\beta$ -diketonate ligands in each complex. Note also that the large molar absorption coefficient obtained for the newly designed  $\beta$ -diketonate ligand indicates that it has a strong ability to absorb light.

**Solution-State PL.** The excitation and emission spectra of **1** and **2** in  $\text{CHCl}_3$  solution ( $c = 1.5 \times 10^{-6} \text{ mol dm}^{-3}$ ) are displayed in Figure 3. The excitation profile of each complex closely mimics that of its corresponding absorption spectrum in the 250–400 nm region, thus demonstrating that energy transfer occurs from the  $\beta$ -diketonate ligands to the  $\text{Eu}^{3+}$  ion. The excitation spectra of **1** and **2** exhibit a broad band between 250 and 400 nm which is attributable to the  $\pi-\pi^*$  transition of the coordinated ligands. The absence of any absorption bands due to the f-f transitions of the  $\text{Eu}^{3+}$  ion proves that luminescence sensitization via excitation of the ligand is effective. The ambient-temperature emission spectra of  $\text{Eu}^{3+}$  complexes **1** and **2** show characteristics of the metal ion emissions in the 550–725 nm region, and exhibit well resolved peaks that are due to the transitions from the metal-centered  $^5\text{D}_0$  excited state to the  $^7\text{F}_J$  ground state multiplet.<sup>6</sup> Maximum peak intensities at 580, 592, 612, 652, and 702 nm were observed for the  $J = 0, 1, 2, 3,$  and  $4$  transitions, respectively, and the  $J = 2$  so-called “hypersensitive” transition is intense.<sup>6</sup> The intensity of the  $^5\text{D}_0 \rightarrow ^7\text{F}_2$  transition (electric dipole) is greater than that of the  $^5\text{D}_0 \rightarrow ^7\text{F}_1$  transition (magnetic dipole), which indicates that the coordination environment of the  $\text{Eu}^{3+}$  ion is devoid of an inversion center. No broad emission band resulting

(27) Nakamura, K.; Hasegawa, Y.; Kawai, H.; Yasuda, N.; Kanehisa, N.; Kai, Y.; Nagamura, T.; Yanagida, S.; Wada, Y. *J. Phys. Chem. A* **2007**, *111*, 3029–3037.

(28) Xu, H.; Wang, L.-H.; Zhu, X.-H.; Yin, K.; Zhong, G.-Y.; Houa, X.-Y.; Huang, W. *J. Phys. Chem. B* **2006**, *110*, 3023–3029.

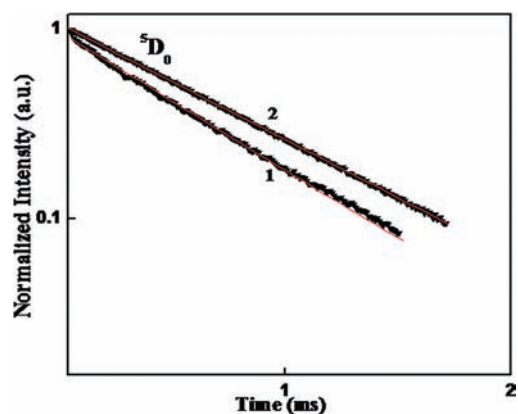
**Table 3.** Radiative ( $A_{\text{RAD}}$ ) and Non-Radiative ( $A_{\text{NR}}$ ) Decay Rates,  $^5\text{D}_0$  Lifetime ( $\tau_{\text{obs}}$ ), Intrinsic Quantum Yield ( $Q_{\text{Eu}}^{\text{Eu}}$ , %), Energy Transfer Efficiency ( $\eta_{\text{sens}}$ , %), and Overall Quantum Yield ( $Q_L^{\text{Eu}}$ , %) for Complexes **1** and **2** in  $\text{CHCl}_3$  Solution and as PMMA Films (**4**–**7**)

complex	$A_{21}$	$\tau_{\text{obs}}$ ( $\mu\text{s}$ )	$A_{\text{RAD}}$ ( $\text{s}^{-1}$ )	$A_{\text{NR}}$ ( $\text{s}^{-1}$ )	$Q_{\text{Eu}}^{\text{Eu}}$ (%)	$Q_L^{\text{Eu}}$ (%)	$\eta_{\text{sens}}$ (%)
<b>1</b>	7.903	$585 \pm 2$	603	1104	35	8	22
<b>2</b>	16.13	$714 \pm 1$	986	413	70	47	66
<b>4</b>	14.53	$764 \pm 1$	934	375	73	79	100
<b>5</b>	15.23	$751 \pm 1$	986	345	74	84	100
<b>6</b>	15.56	$732 \pm 1$	977	390	72	80	100
<b>7</b>	15.01	$762 \pm 1$	960	352	73	83	100

from organic ligand molecules in the blue region can be observed, which indicates that the ligand transfers the absorbed energy effectively to the emitting level of the metal ion. To estimate the relative transition probability of the electric-dipole transition, the relative integrated intensity of the  $^5\text{D}_0 \rightarrow ^7\text{F}_2$  transition with respect to that of the  $^5\text{D}_0 \rightarrow ^7\text{F}_1$  transition band was evaluated<sup>29</sup> ( $A_{21} = A_{\text{ED}}/A_{\text{MD}}$ ;  $A_{\text{ED}}$ , integrated intensity at the electric-dipole transition;  $A_{\text{MD}}$ , integrated intensity at the magnetic-dipole transition). The  $A_{21}$  values for the  $\text{Eu}^{3+}$  complexes are listed in Table 3. The  $A_{21}$  value for complex **2** in the presence of ancillary ligand was considerably larger than that of complex **1** with the carbazole-substituted fluorinated  $\beta$ -diketonate ligand. The introduction of a highly rigid chelating phosphine oxide into the coordination sphere of the  $\text{Eu}^{3+}$ -tris- $\beta$ -diketonate complex would lead to an effective reduction of the symmetry around the  $\text{Eu}^{3+}$  ion. Briefly, the presence of the chelating phosphine oxide increases the luminescent intensity of the hypersensitive transition of the  $\text{Eu}^{3+}$  ion. It is easy to understand from Figure 3 that the displacement of the solvent molecules from the complex  $\text{Eu}(\text{CPFHP})_3(\text{C}_2\text{H}_5\text{OH})(\text{H}_2\text{O})$  by the chelating phosphine oxide significantly enhances the luminescent intensity.

The observed luminescence decays ( $\tau_{\text{obs}}$ ) are single exponential functions for chloroform solutions of complexes **1** and **2** at 303 K, thus indicating the presence of only one emissive  $\text{Eu}^{3+}$  center. Typical decay profiles for complexes **1** and **2** are displayed in Figure 4. The somewhat shorter lifetime observed for complex **1** may be due to the dominant non-radiative decay channels associated with vibronic coupling induced by the presence of solvent molecules, as has been well documented for several hydrated europium  $\beta$ -diketonate complexes.<sup>12</sup> In the case of  $\text{Eu}^{3+}$ , the energy gap between the luminescent state and the ground state manifold is approximately  $12,000 \text{ cm}^{-1}$ . Thus, relatively efficient coupling of the  $\text{Eu}^{3+}$  excited states occurs to the third vibrational overtone of the proximate OH oscillators ( $\nu_{\text{OH}} \sim 3300\text{--}3500 \text{ cm}^{-1}$ ) which is consistent with the observed quenching of  $\text{Eu}^{3+}$  luminescence.<sup>30</sup> On the other hand, because of the absence of non-radiative decay pathways, longer lifetime values have been observed for complex **2** in which the solvent molecules have been replaced by the chelating phosphine oxide.

To gain a better understanding of the luminescence efficiencies of  $\text{Eu}^{3+}$  complexes **1** and **2**, it was appropriate to analyze the emissions in terms of eq 2 (below) where

**Figure 4.** Experimental luminescence decay profiles for complexes **1** and **2** in  $\text{CHCl}_3$  solution ( $c = 1.5 \times 10^{-6} \text{ mol dm}^{-3}$ ) monitored at approximately 612 nm and excited at the maximum emission wavelengths.

$Q_L^{\text{Eu}}$  and  $Q_{\text{Eu}}^{\text{Eu}}$  represent the ligand-sensitized and intrinsic luminescence quantum yields of  $\text{Eu}^{3+}$ ;  $\eta_{\text{sens}}$  represents the efficiency of the ligand-to-metal energy transfer and  $\tau_{\text{obs}}/\tau_{\text{rad}}$  are the observed and radiative lifetimes of  $\text{Eu}^{3+}$  ( $^5\text{D}_0$ ).<sup>31</sup>

$$Q_L^{\text{Eu}} = \eta_{\text{sens}} \times Q_{\text{Eu}}^{\text{Eu}} = \eta_{\text{sens}} \times (\tau_{\text{obs}}/\tau_{\text{rad}}) \quad (2)$$

The intrinsic quantum yields of  $\text{Eu}^{3+}$  could not be determined experimentally upon direct f-f excitation because of very low absorption intensity.<sup>1c</sup> Therefore, the radiative lifetimes of  $\text{Eu}^{3+}$  ( $^5\text{D}_0$ ) have been calculated from eq 3,<sup>31,32</sup> where  $n$  represents the refractive index (1.45 for  $\text{CHCl}_3$ ),  $A_{\text{MD},0}$  is the spontaneous emission probability for the  $^5\text{D}_0 \rightarrow ^7\text{F}_1$  transition in vacuo ( $14.65 \text{ s}^{-1}$ ), and  $I_{\text{tot}}/I_{\text{MD}}$  signifies the ratio of the total integrated intensity of the corrected  $\text{Eu}^{3+}$  emission spectrum to the integrated intensity of the magnetic dipole  $^5\text{D}_0 \rightarrow ^7\text{F}_1$  transition:

$$1/\tau_{\text{rad}} = A_{\text{MD},0} \times n^3 (I_{\text{tot}}/I_{\text{MD}}) \quad (3)$$

The intrinsic quantum yields for  $\text{Eu}^{3+}$  complexes **1** and **2** have been estimated from the ratio  $\tau_{\text{obs}}/\tau_{\text{rad}}$ , and the pertinent values are listed in Table 3.<sup>31</sup> The overall quantum yields ( $Q_L^{\text{Eu}}$ ), radiative ( $A_{\text{RAD}}$ ) and non-radiative ( $A_{\text{NR}}$ ) decay rates, and energy transfer efficiencies ( $\eta_{\text{sens}}$ ) for **1** and **2** are presented in Table 3. The overall quantum yields of ligand-sensitized europium luminescence for complexes **1** and **2** in  $\text{CHCl}_3$  solution have been calculated by a relative method using quinine sulfate as the standard.<sup>19</sup> At room temperature, the substitution of

(29) Harada, T.; Nakano, Y.; Fujiki, M.; Naito, M.; Kawai, T.; Hasegawa, Y. *Inorg. Chem.* **2009**, *48*, 11242–11250.

(30) (a) Ramya, A. R.; Reddy, M. L. P.; Cowley, A. H.; Vasudevan, K. V. *Inorg. Chem.* **2010**, *49*, 2407–2415. (b) Werts, M. H. V. *Sci. Prog.* **2005**, *88*, 101–131.

(31) Shavaleev, N. M.; Eliseeva, S. V.; Scopelliti, R.; Bünzli, J.-C. G. *Inorg. Chem.* **2010**, *49*, 3927–3936.

(32) Werts, M. H. V.; Jukes, R. T. F.; Verhoeven, J. W. *Phys. Chem. Chem. Phys.* **2002**, *4*, 1542–1548.

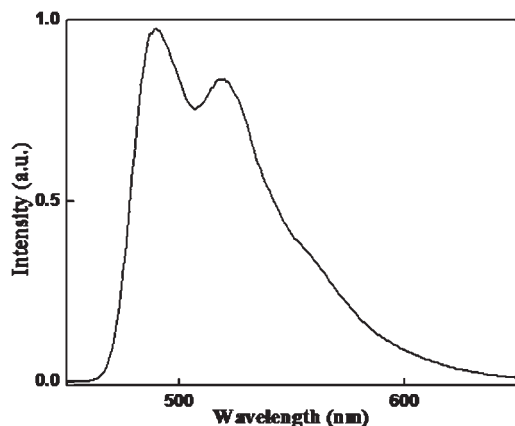


**Figure 5.** Phosphorescence spectrum of  $\text{Gd}(\text{CPFHP})_3(\text{H}_2\text{O})(\text{C}_2\text{H}_5\text{OH})$  at 77 K.

solvent molecules in the  $\text{Eu}^{3+}$ -tris- $\beta$ -diketonate complex by the chelating phosphine oxide, DDXPO, results in an increase in the  $^3\text{D}_0$  luminescence lifetime from  $585 \pm 2$  to  $714 \pm 0.5 \mu\text{s}$  and an approximately 6-fold enhancement in the absolute quantum yield (8 to 47%) in chloroform solution. To achieve bright luminescence, the ligands must protect the  $\text{Eu}^{3+}$  ion from non-radiative deactivation (term  $Q_{\text{Eu}}^{\text{Eu}}$ ), and provide efficient light harvesting and energy transfer (term  $\eta_{\text{sens}}$ ). The substantial contribution of the chelating phosphine oxide to the overall sensitization of the  $\text{Eu}^{3+}$ -centered luminescence in **2** is confirmed by (i) an increase of the intrinsic quantum yield by a factor of 2.3 which results from removal of the quenching effect of the O–H vibrations, and (ii) the significant enhancement of  $\eta_{\text{sens}}$  from 22 to 66%.

To investigate the PL mechanism of the  $\text{Eu}^{3+}$  complexes, it was desirable to determine the energy levels of relevant electronic states of the ligands. The singlet ( $S_1$ ) energy levels of CPFHP and the chelating phosphine oxide, DDXPO, were estimated by referring to the upper wavelengths of the UV–vis absorption edges of the  $\text{Gd}(\text{CPFHP})_3(\text{H}_2\text{O})(\text{C}_2\text{H}_5\text{OH})$  and  $\text{Gd}(\text{NO}_3)_3(\text{DDXPO})$  complexes. The triplet ( $T_1$ ) energy levels were calculated by referring to the lower wavelength emission edges of the corresponding phosphorescence spectra of complexes  $\text{Gd}(\text{CPFHP})_3(\text{H}_2\text{O})(\text{C}_2\text{H}_5\text{OH})$  (Figure 5) and  $\text{Gd}(\text{NO}_3)_3(\text{DDXPO})$ . Thus, the  $S_1$  and  $T_1$  values for CPFHP were found to be  $24,630 \text{ cm}^{-1}$  and  $20,750 \text{ cm}^{-1}$ , respectively. The  $S_1$  ( $31,850 \text{ cm}^{-1}$ ) and  $T_1$  ( $23,470 \text{ cm}^{-1}$ ) levels for DDXPO were taken from our earlier publication.<sup>6f</sup> The triplet energy level of the CPFHP ligand appears at appreciably higher energy than that of the  $^5\text{D}_0$  state of  $\text{Eu}^{3+}$ , thus indicating that the newly designed  $\beta$ -diketonate ligand can act as an antenna for the photosensitization of the  $\text{Eu}^{3+}$  ion. On the other hand, the  $^5\text{D}_1$  emitting state of  $\text{Eu}^{3+}$  ( $18,800 \text{ cm}^{-1}$ ) is found to be critically close to the triplet state of the CPFHP ligand, which can lead to the thermally assisted back-energy transfer from the central core.<sup>33</sup> However, the triplet energy level of the chelating phosphine oxide, DDXPO ( $23,470 \text{ cm}^{-1}$ ), is appropriate for efficient energy transfer with all the  $^5\text{D}_2$ ,  $^5\text{D}_1$ , and  $^5\text{D}_0$  energy levels of  $\text{Eu}^{3+}$ . Therefore, the PL mechanism for

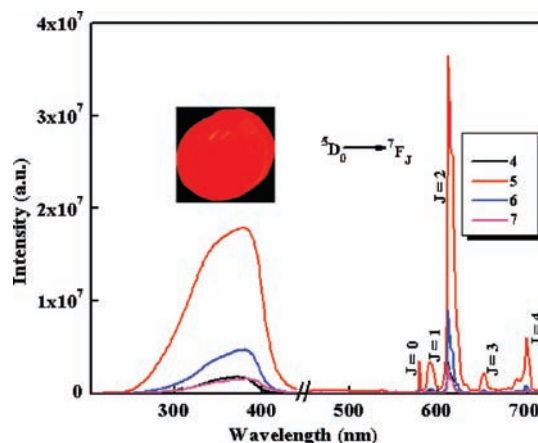


**Figure 6.** Excitation and emission spectra of PMMA films doped with 2.5, to 15% (w/w) of  $\text{Eu}(\text{CPFHP})_3(\text{DDXPO})$ . The data were recorded at 303 K.

the  $\text{Eu}^{3+}$  complexes is proposed to involve a ligand-sensitized luminescence process (antenna effect).<sup>4</sup>

**Photophysical Properties of  $\text{Eu}^{3+}$  Complexes Doped in PMMA Polymer Films.** Lanthanide complexes incorporated into polymer matrixes represent a new class of materials that offer the characteristics of both complexes and polymers, thus making them ideal candidates for use in wide range of new technologies.<sup>15</sup> In the present manuscript, we describe the incorporation of a newly designed, highly luminescent complex into PMMA, a well-known, low-cost, easily prepared polymer of excellent optical quality. Figure 6 shows the excitation spectra of the PMMA polymer films doped with  $\text{Eu}(\text{CPFHP})_3(\text{DDXPO})$  at different concentrations [2.5 (**4**), 7.5 (**5**), 10 (**6**), and 15% (**7**) (w/w)] and recorded at 303 K in the spectral range of 250 to 480 nm, by monitoring the emission at 612 nm. The excitation spectra are dominated by an intense broad band in the 250 to 400 nm region, which can be assigned to absorptions of both the PMMA polymer and the organic chromophore. Of particular note is the observation that the excitation maximum of the spectra is red-shifted as compared to the solution phase spectra. This can be attributed to the considerable interaction of the ligands with PMMA matrix. The emission spectra of PMMA doped with  $\text{Eu}(\text{CPFHP})_3(\text{DDXPO})$  at a variety of concentrations [2.5 (**4**), 7.5 (**5**), 10 (**6**), and 15% (**7**) (w/w)] and excited at 370 nm exhibit five emission bands that are assigned to the characteristic  $^5\text{D}_0 \rightarrow ^7\text{F}_J$  ( $J = 0-4$ ) transitions of the  $\text{Eu}^{3+}$  ion. As displayed in Figure 6, the luminescent intensity of the  $\text{Eu}^{3+}$  emission at 612 nm increases with increasing  $\text{Eu}^{3+}$  content and reaches a maximum at a  $\text{Eu}^{3+}$  content of 7.5%. A further increase in the  $\text{Eu}^{3+}$  content decreases the luminescent intensity. The energy transfer between the lanthanide ions themselves is a non-radiative process, which accounts for the decrease in the  $\text{Eu}^{3+}$  emission, especially at high  $\text{Eu}^{3+}$  content (**6** and **7**).<sup>6i,34</sup> The transition of highest intensity is dominated by the hypersensitive  $^5\text{D}_0 \rightarrow ^7\text{F}_2$  transition at approximately 612 nm, which implies that the  $\text{Eu}^{3+}$  ion does not occupy a site with inversion symmetry. Moreover, the presence of only one sharp peak in the region of the  $^5\text{D}_0 \rightarrow ^7\text{F}_0$  transition

(33) Armaroli, N.; Accorsi, G.; Barigelletti, F.; Couchman, S. M.; Fleming, J. S.; Harden, N. C.; Jeffery, J. C.; Mann, K. L. V.; McCleverty, J. A.; Rees, L. H.; Starling, S. R.; Ward, M. D. *Inorg. Chem.* **1999**, *38*, 5769–5776.

(34) (a) Parra, D. F.; Mucciccolo, A.; Brito, H. F. *J. Appl. Polym. Sci.* **2004**, *94*, 865–870. (b) Li, Q.; Li, T.; Wu, J. *J. Phys. Chem. B* **2001**, *105*, 12293–12296.



at 580 nm suggests the occurrence of a unique chemical environment around the  $\text{Eu}^{3+}$  ion of symmetry type  $C_s$ ,  $C_n$ , or  $C_{nv}$ . It is well-known that the magnetic-dipole transition  ${}^5\text{D}_0 \rightarrow {}^7\text{F}_1$  is nearly independent of the ligand field and therefore can be used as an internal standard to account for ligand differences. The electric-dipole transition  ${}^5\text{D}_0 \rightarrow {}^7\text{F}_2$ , the so-called hypersensitive transitions, is sensitive to the symmetry of the coordination sphere. The intensity ratio of the magnetic-dipole transition to the electric-dipole transition in the lanthanide complex measures the symmetry of the coordination sphere.<sup>15c</sup> The intensity ratios ( $A_{21}$ ) of the  ${}^5\text{D}_0 \rightarrow {}^7\text{F}_2$  transition to the  ${}^5\text{D}_0 \rightarrow {}^7\text{F}_1$  transition in the Eu/PMMA were shown in Table 3. The intensity ratio of the transitions of  ${}^5\text{D}_0 \rightarrow {}^7\text{F}_2$  to  ${}^5\text{D}_0 \rightarrow {}^7\text{F}_1$  is 15.23 for the complex **2** when incorporated into the PMMA matrix (7.5%). These results suggest that, when the Eu complex is incorporated into the microcavities of the polymer matrix, the  $\text{Eu}^{3+}$  ions exhibit different local environments because of the influence of the surrounding polymer. The symmetry of the coordination sphere for the  $\text{Eu}^{3+}$  ions changes moderately in the Eu/PMMA as compared to the pure precursor complex. When incorporated into the microcavities of the PMMA matrix, however, the complexes exhibit disorder of a certain magnitude. Under the influences of the electric field of the surrounding ligands, the distortion of the symmetry around the  $\text{Eu}^{3+}$  ion by the capping PMMA results in the polarization of the  $\text{Eu}^{3+}$ , which increases the probability for electric-dipole, allowed transition. The influences of PMMA on the coordinative environment of the  $\text{Eu}^{3+}$  ions changes the energy-transfer probabilities of the electric-dipole transitions, accounting for the increases in luminescent intensity of the 612 peak.

The luminescence decay curves of the doped films were obtained by monitoring the emission at the hypersensitive  ${}^5\text{D}_0 \rightarrow {}^7\text{F}_2$  transition (612 nm) and excitation at 370 nm (Supporting Information, Figure S5). These data were adjusted with a first-order exponential decay function, and the lifetime values ( $\tau$ ) of the emitter  ${}^5\text{D}_0$  level of the doped systems were determined and are listed in Table 3. All  $\tau$  values for the doped polymer systems are higher than that of the hydrated  $\text{Eu}^{3+}$  complex, thus indicating that radiative processes are operative in all the doped polymer films because of the absence of multiphonon relaxation by coupling with the OH oscillators from the  $\text{Eu}(\text{CPFHP})_3(\text{C}_2\text{H}_5\text{OH})(\text{H}_2\text{O})$  complex. On the other hand, the  ${}^5\text{D}_0$  lifetime of the doped films was not obviously influenced by the embedded PMMA.

The overall quantum yields ( $Q_L^{\text{Eu}}$ ) determined by the absolute method, radiative ( $A_{\text{RAD}}$ ) and non-radiative ( $A_{\text{NR}}$ ) decay rates, intrinsic quantum yields ( $Q_{\text{Eu}}^{\text{Eu}}$ ), and energy transfer efficiencies ( $\eta_{\text{sens}}$ ) of the PMMA films doped with  $\text{Eu}(\text{CPFHP})_3(\text{DDXPO})$  at different doping concentrations are presented in Table 3. All the PMMA doped films exhibit excellent overall quantum yield values, ranging from 79 to 84%. This range is comparable to that reported recently for luminescent europium  $\beta$ -diketonate complexes doped in PMMA matrices.<sup>18a,24,35</sup> Furthermore, the substantial increase in  $\eta_{\text{sens}}$  (from 66% in complex

**2** to 100% in luminescent PMMA films) on going from  $\text{CHCl}_3$  to PMMA is consistent with the elimination of collisional quenching of the ligand triplet state in the polymer matrix. It is well-known that the efficiency of the intermolecular energy transfer is strongly dependent on the distance between the donor and acceptor.<sup>36</sup> According to this point of view, it is suggested that for the present system, the PMMA molecule, because of its long chain, has the capability to enwrap the  $\text{Eu}(\text{CPFHP})_3(\text{DDXPO})$  complex and keeps the acceptor and donor close. In such a case, energy can be transferred efficiently from ligand to  $\text{Eu}^{3+}$ , resulting in the enhancement of intrinsic  $\text{Eu}^{3+}$  emission of a  $\text{Eu}(\text{CPFHP})_3(\text{DDXPO})$ . Thus the preserved rigidity in the complex structure in PMMA could be the origin of the enhanced overall quantum yield. Strikingly, the present work shows the role of DDXPO is much more significant in PMMA than in chloroform, with europium complex **2** doped in a PMMA polymer matrix (**4–7**) displaying markedly higher  $Q_{\text{Eu}}^{\text{Eu}}$  values (72 to 74%) than **1** and **2**. Again, this may arise from the enhanced encapsulation of  $\text{Eu}^{3+}$  center minimizing the detrimental effect of the C–H oscillators in the PMMA matrix that potentially provide non-radiative decay pathways for the  $\text{Eu}^{3+}$  excited state.

## Conclusions

In summary, we have designed, synthesized, and characterized a novel eight-coordinate, highly luminescent lanthanide complex that utilizes a fluorinated carbazole-substituted  $\beta$ -diketonate in conjunction with the ancilliary ligand, 4,5-bis(diphenylphosphino)-9,9-dimethylxanthene oxide, for indirect excitation of the europium metal center. The new complex displays efficient sensitized luminescence in chloroform solution ( $\eta_{\text{sens}} = 66\%$ ) with a quantum yield of 47%. Additionally, the newly designed europium complex was incorporated into PMMA polymer films, which were shown to exhibit exceptionally high PL quantum yields (79–84%). This implies that the PMMA with high molecular weight enwraps the  $\text{Eu}^{3+}$  complex and keeps the donor and acceptor close, which results in the effective intermolecular energy transfer and, consequently, the high sensitization efficiency. In conclusion, the PMMA films doped with the  $\text{Eu}^{3+}$ - $\beta$ -diketonate complex show promising PL efficiency and therefore have potential applications as polymer light-emitting diodes and active polymer optical fibers.

**Acknowledgment.** The authors acknowledge financial support from the Department of Science & Technology (SR/S1/IC-36/20073) and the Council of Scientific and Industrial Research (NWP0023). D.B.A.R. thanks the University Grants Commission, New Delhi for the award of Senior Research Fellowship. A.H.C. thanks the Robert A. Welch Foundation (Grant F-0003) for generous financial support as well as well as the National Science Foundation (Grant 0741973).

**Supporting Information Available:** Further details are given in Figures S1–S5, and crystallographic data is given in CIF format. This material is available free of charge via the Internet at <http://pubs.acs.org>.

(35) Hasegawa, Y.; Kawai, H.; Nakamura, K.; Yasuda, N.; Wada, Y.; Yanagida, S. *J. Alloys Compd.* **2006**, *408*, 669–674.

(36) Foster, T. *Ann. Phys.* **1948**, *2*(1–2), 55–75.